

## RESEARCH PAPER

# Substrate-perforated and compact ultra-wideband antenna with WLAN band rejection

WESSAM ZAYD SHAREEF<sup>1</sup>, ALYANI ISMAIL<sup>2</sup> AND ADAM R.H. ALHAWARI<sup>1</sup>

*This paper presents a designed notched band ultra-wideband (UWB) printed antenna using coplanar waveguide-fed configuration. Simple technique of perforating the substrate and modifying the ground plane and radiator patch was used to achieve UWB for the designed antenna at smaller structure. Narrow arch-shaped slot was introduced to the patch of the proposed antenna to obtain the band rejection function around the 5.4 GHz frequency to avoid the interference with WLAN applications. The proposed antenna was fabricated and the measurement result is found in well agreement with the simulation result. In addition to the acquirable UWB bandwidth, the designed antenna is capable to exhibit high radiation efficiency and omni-directional pattern.*

**Keywords:** Antenna design, Modeling and Measurements, Antennas and Propagation for Wireless Systems

Received 14 January 2014; Revised 26 April 2014; Accepted 15 May 2014; first published online 13 June 2014

## I. INTRODUCTION

Tremendous developments in the wireless communications applications (mobile internet, audio/video streaming, etc.) in the last couple of decades, led to urgent need to a new technology that has the ability to transfer a vast data rate. The existing of ultra-wideband (UWB) technology gives the chance to address these issues. The mechanism of the UWB technology is based on transmits and receives of very short electromagnetic pulses over a large portion of the frequency spectrum at low radiation power [1]. This mechanism offers a number of advantages such as multipath immunity, high data rate, low-power consumption, and less hardware complexity systems [2]. As the case in traditional wireless communication systems, antenna plays an essential role in the UWB systems performance. According to the FCC report in 2002, an UWB antenna should operate over the bandwidth from 3.1 to 10.6 GHz, evaluated by return loss less than  $-10$  dB [3]. Additionally, an omni-directional radiation pattern is desirable for wireless communications, since it enables freedom in the receiver and transmitter locations.

Various designs of horn [4], biconical [5], and planar plate monopole antennas [6–8], have been proposed to cover the UWB bandwidth. However, these types of antennas have three-dimensional (3D) structural geometry and large in size, which makes them incompatible with portable devices. Other

approaches gave more attention for printed antennas [9–11]. This is due to their small size, simple profile, low cost, and easy to fabricate. Miniaturization and increasing the impedance bandwidth are one of the most important design requirements of UWB-printed antennas. A lot of effort has been devoted to achieve these requirements. Some designers use a rectangular capacitive coupled feed in order to solve the large probe reactance problem caused by the required long probe pin in the thick substrate layer [12]. Via holes are also used to adjust the input impedance of the UWB antennas [13, 14]. In the same context, introducing a very narrow slits near the feeding point of the staircase patch radiator [15] and adding parasitic elements close to the radiator patch [16, 17] were used as another techniques to improve the impedance bandwidth of the compact printed structures. The use of the mentioned techniques adds more complexity to the antennas and makes them very difficult and costly to fabricate.

Moreover, the utilization of a large chunk of spectrum frequency by the UWB technology increases the possibility of having the electromagnetic interference with some of the existing wireless networking standards, such as HIPERLAN/2 in Europe (5.15–5.35 and 5.47–5.725 GHz) and IEEE 802.11a in the USA (5.15–5.35 and 5.725–5.825 GHz) [18]. Consequently, rejection of a particular sub-band becomes an important UWB system design requirements. In case of using individual microwave band-stop filter to reject the undesirable sub-band, this contributes to additional insertion losses, cost, and larger size to the system. A more beneficial solution to overcome this problem is by employing an UWB antenna with band-notch capability [19–21].

In this paper, a compact size, low-cost, and coplanar waveguide (CPW)-fed patch UWB antenna with sub-band rejection capability was proposed. The main advantage of using the

<sup>1</sup>Wireless and Photonics Research Centre, Department of Computer and Communication Systems Engineering, Faculty of Engineering, Universiti Putra Malaysia, Selangor, Malaysia. Phone: +6017 3939 414

<sup>2</sup>Institute of Advanced Technology, Universiti Putra Malaysia, Selangor, Malaysia

**Corresponding author:**

Adam R.H. Alhawari

Email: adamreda@upm.edu.my

CPW-fed method over the conventional ones such as microstrip and coaxial is that; by applying CPW-fed configuration both the radiating element and the ground plane are printed on the same side of the dielectric substrate. Therefore, most of the electromagnetic wave travels along the metal patches located on one side of the antenna structure, and less energy is lost in the substrate. Furthermore, new simple techniques of perforating the substrate and using the half-elliptical shapes to configure each of the patch and the ground plane were introduced to increase the impedance bandwidth of the proposed compact antenna. The band rejection characteristic is obtained by employing an arched slot in the patch radiator.

## II. ANTENNA DESIGN

The proposed antenna (Fig. 1) is a printed-circuit antenna using CPW feeding and arched patch on top edges. This

monopole antenna also consists of a semi-circular-shaped patch fed by ungrounded CPW line and half-ellipse-shaped ground planes printed on the same side of the substrate as shown in Fig. 1. The inner line of the CPW is tapered near its connection point with the radiator to improve the impedance matching between them. The antenna substrate was perforated with circular four holes distributed on the unprinted area of the structure. The circular shape of the holes was chosen mainly to simplify drilling for fabrication procedures. An arc-shaped slot is then notched in the radiator in order to achieve the sub-band rejection facility.

As elaborated in Fig. 1, the ground plane of the antenna has also been modified to form a half-ellipse (whose major axis runs parallel to the feed line). This modification of the ground plane affords a wider variation in the wavelength due to gap-width variation between the patch and the ground plane. As such, new resonance frequencies are created leading to increased bandwidth as shown in Fig. 2.

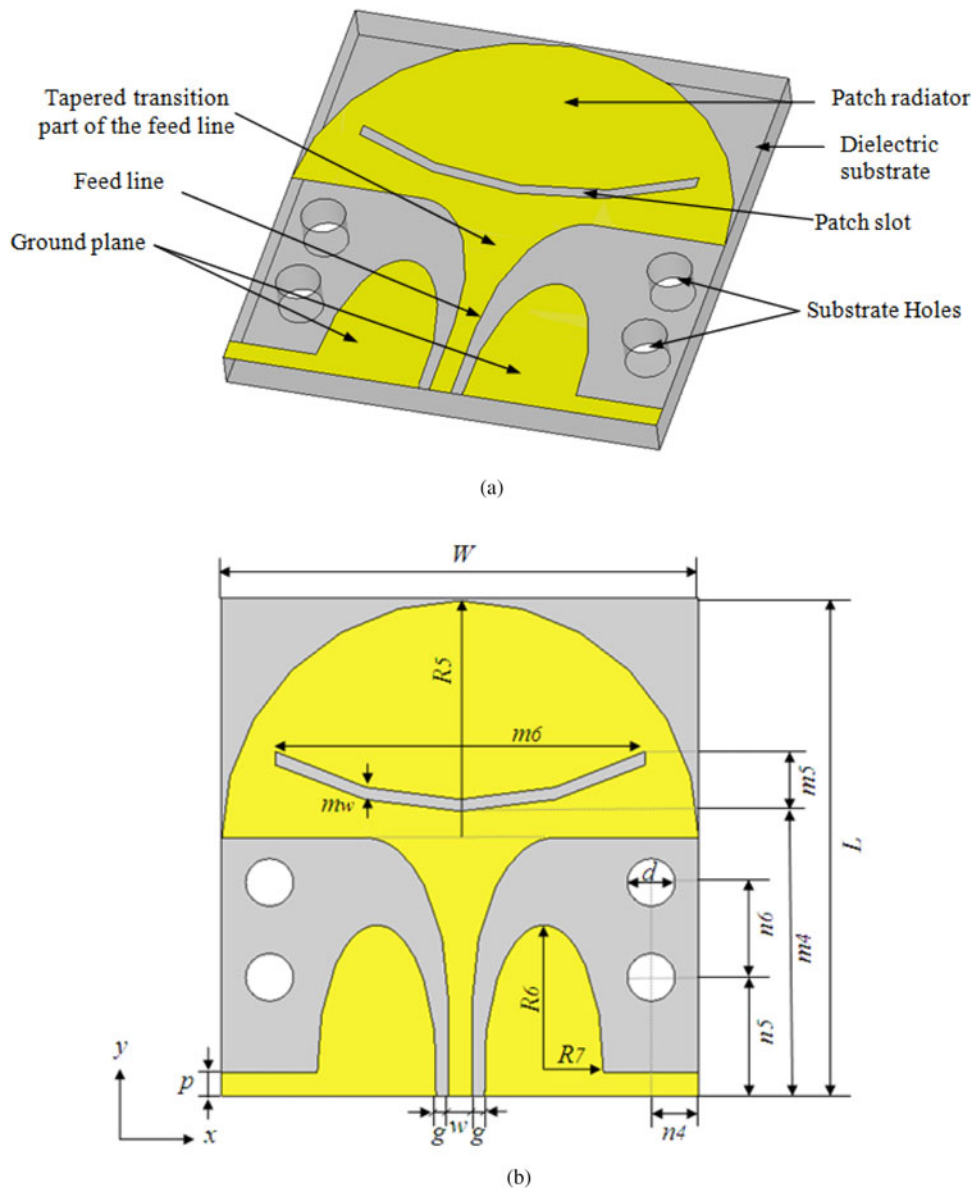


Fig. 1. Configuration of the proposed antenna: (a) prospective view and (b) its parameters.

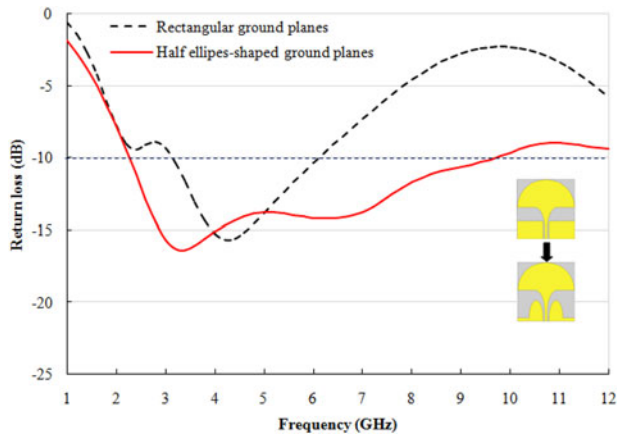


Fig. 2. Simulated return loss of two antennas with the rectangular and half ellipse-shaped ground planes.

Once the effect of the half-elliptical ground plane was analyzed, a pair of circular holes was perforated on either sides of the feed line, within the unprinted area. In Fig. 3, it can be noted that the electrical field vectors become more concentrated at the parts of the ground planes that are near to the radiator after creating the substrate holes. This result in reducing the losses at higher frequency band and further widened the bandwidth at higher frequency band as in Fig. 4.

The copper of the patch is etched to form an arc-shaped slot in the radiating element, in order to obtain a frequency band-notch function. This slot distorts the surface current distribution of the patch, for the antenna to be inoperative at the undesired sub-band as shown in Fig. 5. It can be seen from Fig. 6 that the undesired sub-band rejected at around 5.4 GHz. This phenomenon is associated to the fact that at the slot edges, there is a high surface current concentration at the notch frequency. As such, the impedance nearby the feed point at this frequency is very low, resulting in high reflection at the rejected sub-band.

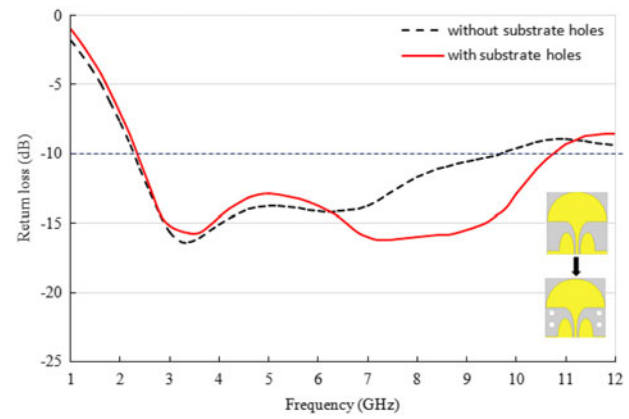


Fig. 4. Simulated return loss of two antennas with and without substrate holes.

### III. PARAMETERS ANALYSIS OF THE PROPOSED ANTENNA

From Fig. 7, when  $R_6$  is 7.1 mm, the observed losses at the higher frequencies are very small, but very high at the lower frequencies. As  $R_6$  is decreased to 5.1 mm, the observed return losses at the higher frequencies get higher. The reason for observed result can be attributed to the fact that as  $R_6$  is increased, the gap between the radiator and the ground plane gets correspondingly narrower, which tends to shorten the electromagnetic wavelengths ( $\lambda$ ), ensuring a reduction in the losses at the higher frequencies. Decreasing  $R_6$  on the other hand widens the gap between the radiator and the ground plane thereby allowing the propagation of electromagnetic waves with longer wavelengths; hence, the lower losses at the lower frequencies. Consequently, the optimized value for  $R_6$  was found to be 6.1 mm, at which the losses at both the lower and higher frequencies are kept at a minimum.

In order to analyze the effect of perforating holes on the unprinted area of the substrate, the proposed antenna was first simulated without any holes. One hole is then perforated

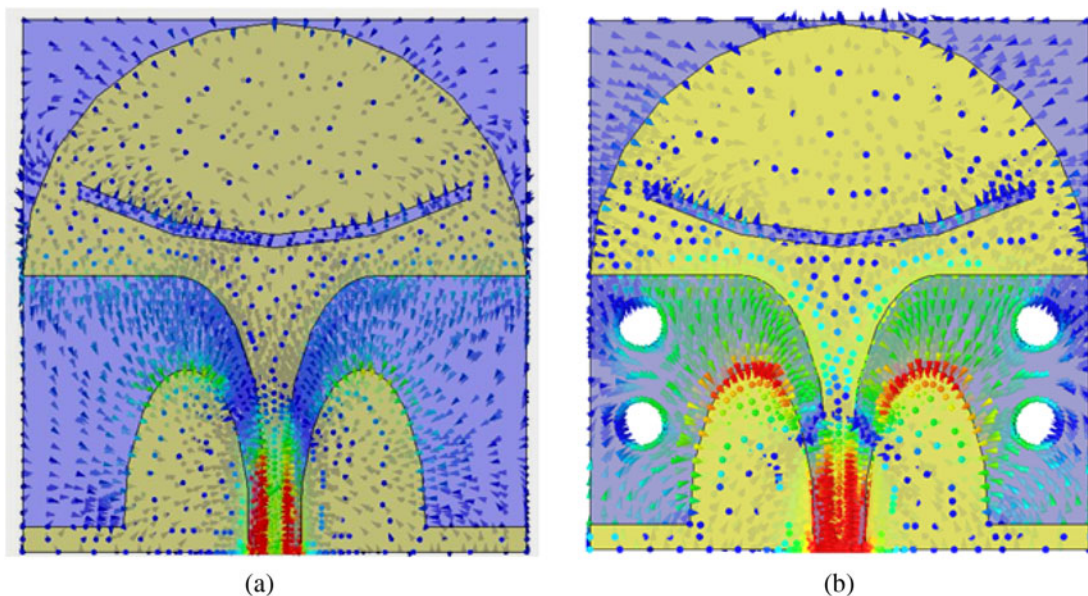


Fig. 3. Electric field distribution: (a) without substrate holes and (b) with substrate holes.

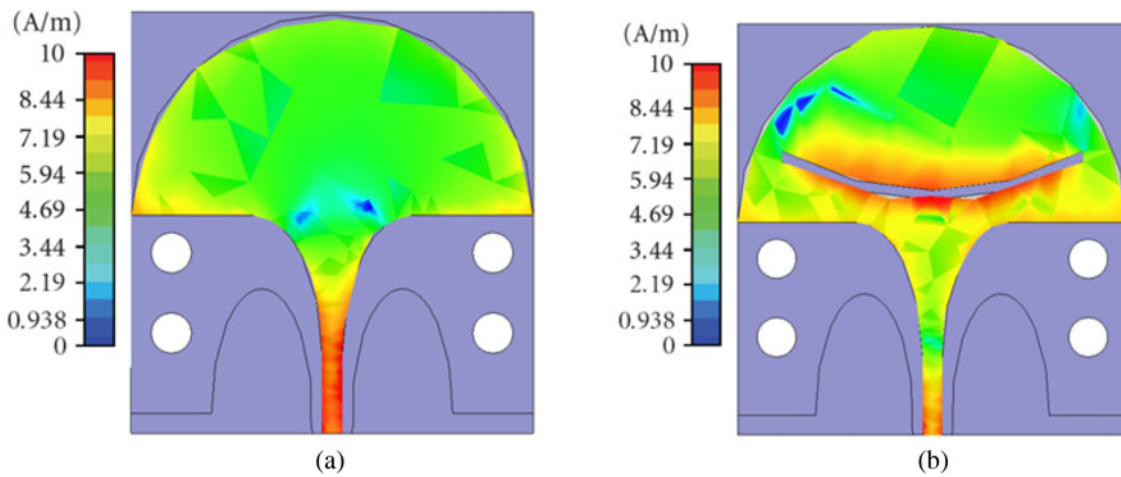


Fig. 5. Surface current distribution at 5.4 GHz: (a) without patch slot and (b) with patch slot.

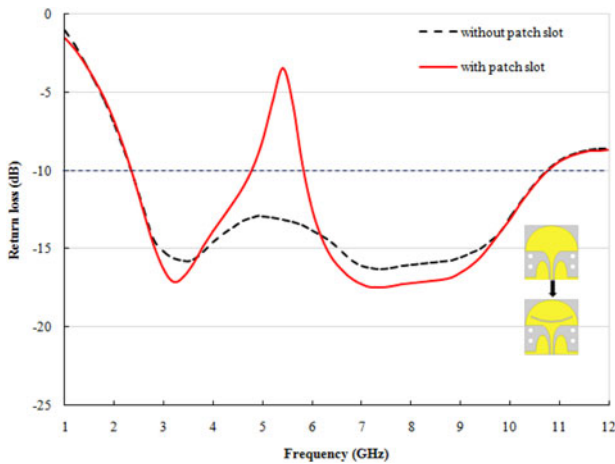


Fig. 6. Simulated return loss of two antennas with and without patch slot.

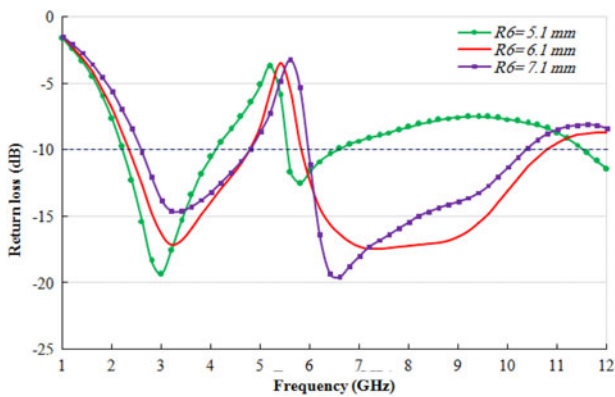


Fig. 7. Simulated return loss with different values of  $R_6$ .

on either sides of the feed line at the unprinted portion. The holes number was then increased to two pairs and then three pairs. When no hole was perforated, the obtained return loss at the higher frequencies was highest. Perforating one hole on either sides (one pair), the  $S_{11}$  at higher frequencies subsided to a considerable degree. Doubling the number of holes (two pairs), it was observed that the higher cut-off frequency of

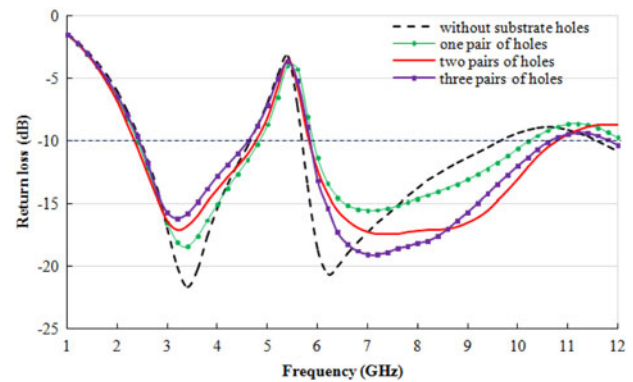


Fig. 8. The number of the substrate holes effect on the designed antenna.

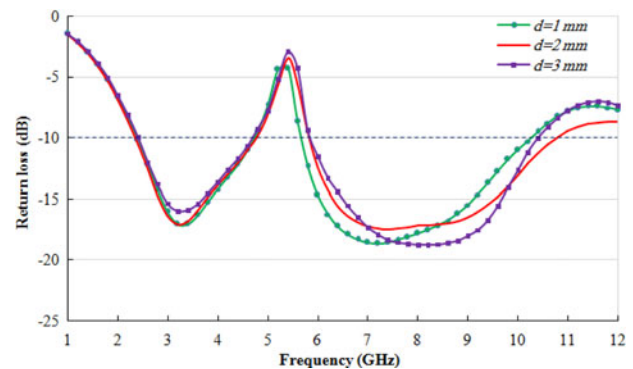


Fig. 9. The diameter of the substrate holes effect.

the bandwidth further shifted upwards as shown in Fig. 8. This phenomenon can be attributed to the fact that, the flowing electromagnetic energy from the radiator element to the ground planes on the substrate surface becomes more concentrated at the parts that responsible to radiate the higher frequencies when the holes are created in the substrate. In this way, the losses are lesser at the higher part of the bandwidth. However, when the number of holes increased to three on each side (three pairs), no significant change is observed. This result is not surprising in that the already existing two holes on each side are sufficient enough to cage the extra energy.

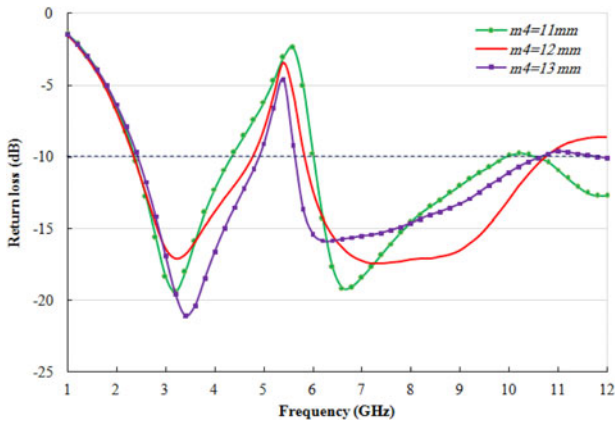


Fig. 10. Simulated return loss for different values of  $m_4$ .

Figure 9 shows the effect of resizing the hole-diameter. When the smallest hole-diameter of 1 mm is used, it is observed that it has the least effect on impedance matching, while a 3 mm hole-diameter has an effect on the lower frequency band. In this way, it is found that hole-diameter of 2 mm exhibits the optimal bandwidth.

In order to investigate the effect of changing the slot position on the notched-band, the distance  $m_4$  as shown in Fig. 1(b) was varied. The return loss curve in Fig. 10 shows that the rejected sub-band is very wide when the slot is shifted downwards, closer to the feed point, while shifting the slot away from the feed point in the  $y$ -direction provides

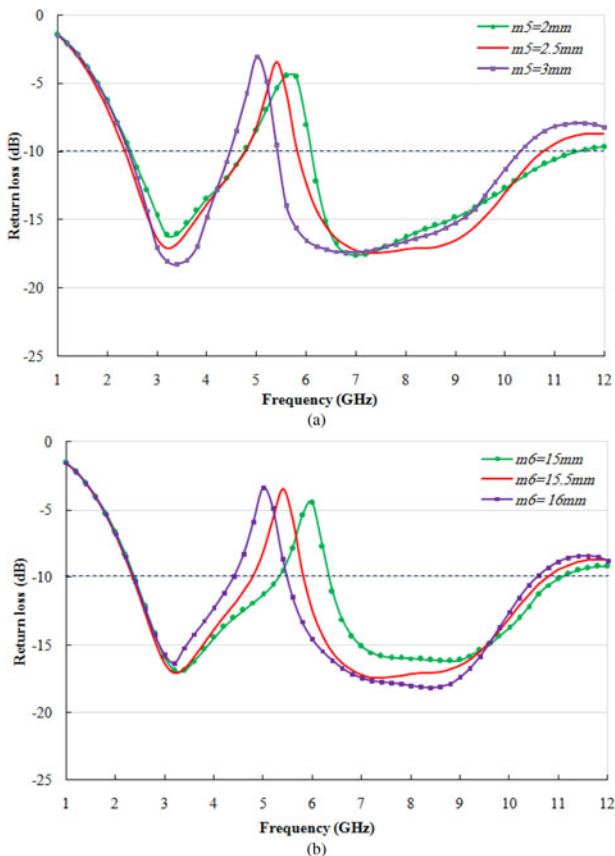


Fig. 11. Simulated return loss for different values of (a)  $m_5$  and (b)  $m_6$ .

Table 1. Optimized dimensions of the proposed antenna.

Parameters	Values (mm)
$W$	20
$L$	21
$w$	1
$g$	0.5
$p$	1
$R_5$	10
$R_6$	6.1
$R_7$	2
$n_4$	2
$n_5$	6
$n_6$	4
$d$	2
$m_4$	12
$m_5$	2.5
$m_6$	15.5
$mw$	0.5

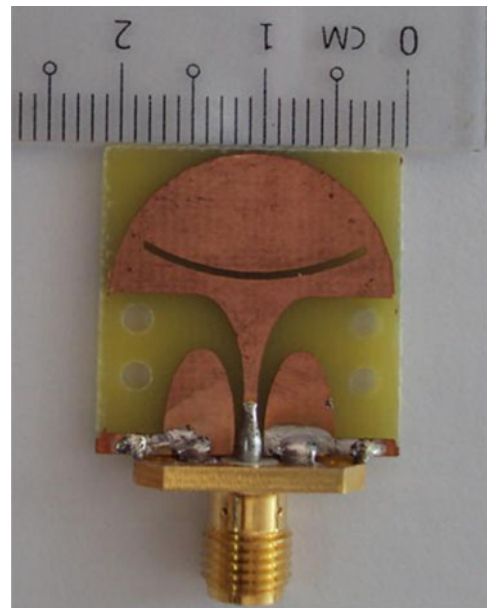


Fig. 12. Photograph of the fabricated antenna.

sharp notched-band with the least rejection ability. From observation, this phenomenon occurs because when the slot is etched near the feed line, whereby the surface current-effect at the fringes of the patch-slot increases significantly. Similarly, shifting the patch-slot further away from the feed point, results in less current-effect at the slot edges. In this way, bringing the slot very close to the feed point produces too wide rejected band.

The effect of the slot length on the band-stop has already been investigated. In the analysis of the effect of varying the patch-slot width  $m_6$  and depth  $m_5$  as shown in Fig. 11, it was found that increasing or decreasing  $m_5$  and/or  $m_6$  results to an increase or decrease in the patch slot length. From Fig. 11(a), it is observed that increasing  $m_5$  causes a shift in the center frequency of the notched-band toward the lower frequencies. Conversely, the center frequency of the notched-band is shifted toward the higher frequencies by decreasing  $m_5$ . A similar phenomenon is observed when  $m_6$  is increased or decreased as shown in Fig. 11(b).

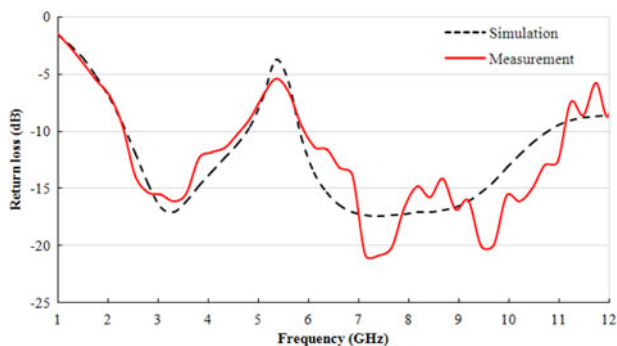


Fig. 13. Simulated and measured return loss result.

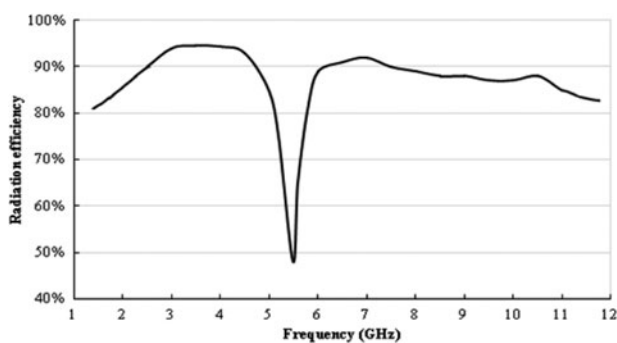


Fig. 14. Radiation efficiency.

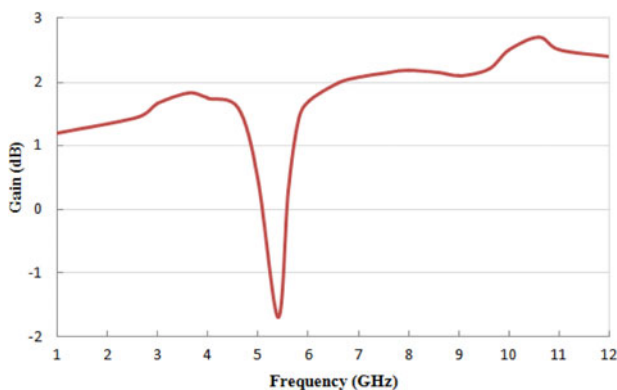


Fig. 15. Gain of the proposed antenna.

#### IV. SIMULATED AND MEASURED RESULTS

The proposed antenna having the dimensions as listed in Table 1 was fabricated and measured as shown in Fig. 12. The measured and simulated return loss values in terms of frequency are compared in Fig. 13. The measured results are in good agreement with the simulation results. The measured impedance bandwidth is about 8.4 GHz starting from 2.45 to 10.9 GHz ( $S_{11} \leq -10$  dB) excluding the notched band from 4.83 to 5.97 GHz. The simulation results show an operational bandwidth starts from 2.6 to 11.2 GHz, in which a frequency band-notch is from 4.88 to 5.8 GHz. The small discrepancy between the simulated and the measured losses at the higher frequencies

which can be attributed to the tolerance in the fabrication process, imperfect soldering, SMA connector effects in the measurement, and the reflection effect of the radiated waves occurs from the surrounding walls, devices, and cables in the measurement which were not taken into account in the simulations.

Figure 14 shows the radiation efficiency of the optimized antenna against frequency. It is evident that the range of antenna radiation efficiency is higher than 85%, excluding the band-notch frequency where the antenna has greatest reduction in the radiation efficiency.

The gain of the proposed antenna is presented in Fig. 15. The compact size of the antenna is a factor that lowers the gain for the proposed antenna. It can be seen that the sharp decrease of antenna gain in the notched frequency band at 5.5 GHz and it is at the maximum values for higher frequencies.

The antenna lies in the  $x$ - $y$  plane, and it is  $y$ -polarized because it is feed in the  $y$ -direction. Therefore, the  $H$ -plane for this antenna is  $x$ - $z$ , and the  $E$ -plane is  $y$ - $z$ . The simulated radiation patterns for the designed antenna at 3 – 10.5 GHz are plotted in Fig. 16. It is clearly seen from the figure that in the  $E$ -plane antenna provides almost monopole-like radiation patterns in the entire band with little deterioration at higher frequencies. In the  $H$ -plane, the antenna exhibits the omni-directional radiation pattern from 3 to 10 GHz, and then starts to produce four major lobes at 10.5 GHz. These changes are due to the increase of the antenna size electrically related to the higher frequencies, as the antenna size starts to leave the monopole antenna behavior at the higher frequencies (more than 10.6 GHz) which are considered out of the allocated bandwidth for the UWB wireless communications.

#### V. CONCLUSION

In this work, CPW-fed printed antenna with band rejection capability has been designed for wireless UWB communications portable devices. The antenna design was emanated from the equivalent conventional rectangular patch antenna. By modifying each of the radiating patch and ground plane, the bandwidth of the proposed antennas has been improved. Moreover, a new technique of perforating the dielectric substrate with two pairs of holes has been employed to widen the impedance bandwidth at higher frequencies. By introducing an arch-shaped slot in the antennas radiator, the band stop characteristic was obtained.

The proposed UWB antenna was developed and analyzed by a 3D electromagnetic simulator (CST Microwave Studio, 2013) [22]. To confirm the simulation results, the proposed antenna was fabricated on the FR-4 substrate with dielectric constant of 4.4 and the experimental measurement was carried out using a vector network analyzer (Anritsu 37347D) in room environment. The analysis indicated a fairly good agreement between simulation and measurement. The measured bandwidth of the proposed CPW-fed UWB antenna showed that this antenna has operational bandwidth starting from 2.45 to 10.9 GHz with return loss better than  $-10$  dB excluding the notched band from 4.83 to 5.97 GHz. The overall size of the designed antenna is  $20 \times 21 \times 1.6$  mm<sup>3</sup>. In comparison to the antennas that have been reported in [16, 23, 24], the proposed antenna has a reduction in the surface area of 67, 46, and 74%, respectively. The techniques of modifying the radiator patch and ground

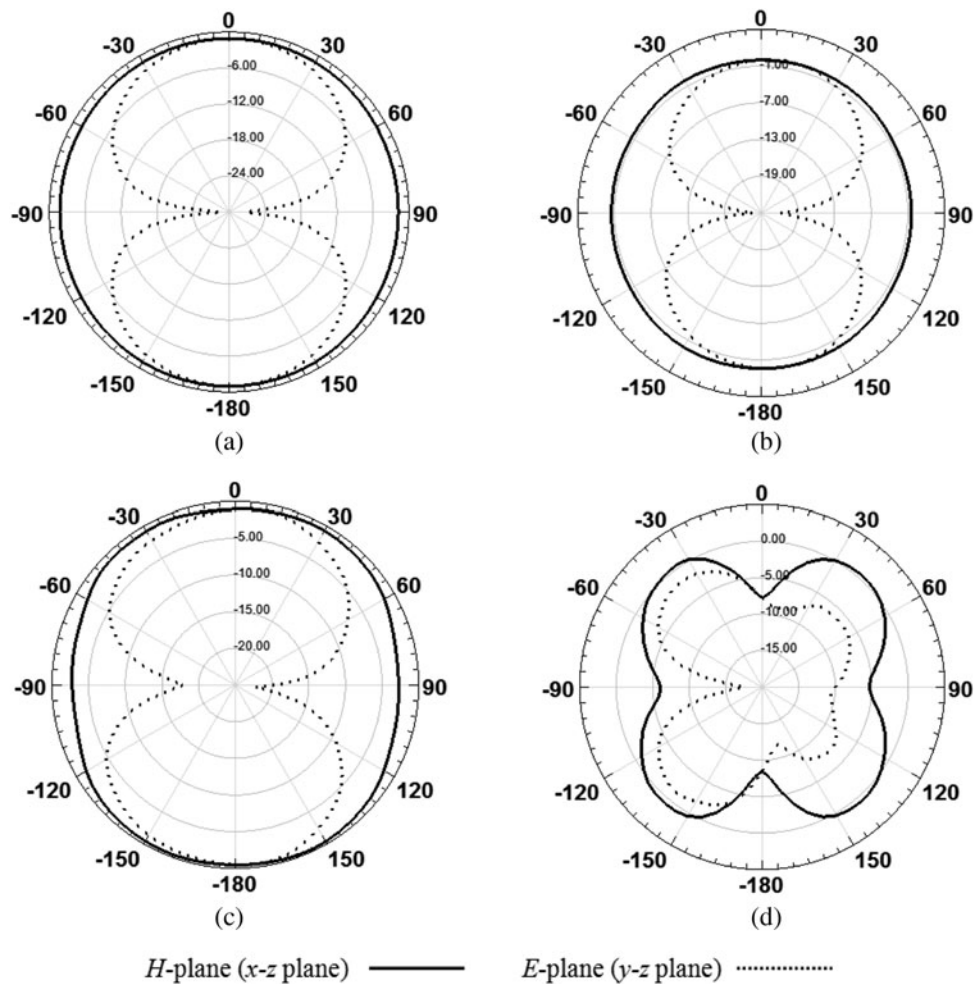


Fig. 16. Radiation pattern at: (a) 4 GHz, (b) 7 GHz, (c) 9 GHz, and (d) 10.5 GHz.

plane, as well as perforation of the substrate has helped to achieve the UWB band characteristics with compact size for the proposed UWB antenna. In addition, the advantages of simple structure, single side print, and compact size make this antenna a suitable choice for modern UWB communication systems.

## REFERENCES

- [1] Lee, J.S.; Nguyen, C.: Novel low-cost ultra-wideband, ultra-short-pulse transmitter with MESFET impulse-shaping circuitry for reduced distortion and improved pulse repetition rate. *IEEE Microw. Wirel. Compon. Lett.*, **11** (2001), 208–210.
- [2] Fontana, R.J.: Recent system applications of short-pulse ultrawideband technology. *IEEE Trans. MTT*, **52** (2004), 2087–2104.
- [3] Anon: FCC first report and order on ultra-wideband technology, February 2002.
- [4] Dehdasht-Heydari, R.; Hassani, H.R.; Mallahzadeh, A.R.: Quad ridged horn antenna for UWB applications. *Prog. Electromagn. Res.*, **79** (2008), 2–38.
- [5] Ghannoum, H.S.; Roblin, C.; Sibille, A.: Biconical antennas for intrinsic characterization of the UWB channel. *IEEE International Workshop, IWAT* (2005), 101–104.
- [6] Dastranj, A.A.; Imani, A.; Hassani, H.R.: V-shaped monopole antenna for broadband applications. *Prog. Electromagn. Res. C*, **1** (2008), 45–54.
- [7] Lamultree, S.; Phongcharoenpanich, C.: Bidirectional ultra-wideband antenna using rectangular ring fed by stepped monopole. *Prog. Electromagn. Res.*, **85** (2008), 227–242.
- [8] Zhou, H.J.; Liu, Q.Z.; Yin, Y.Z.; Wei, W.B.: Study of the band-notch function for swallow-tailed planar monopole antennas. *Prog. Electromagn. Res.*, **77** (2007), 55–65.
- [9] Lim, K.S.; Nagalingam, M.; Tan, C.P.: Design and construction of microstrip UWB antenna with time domain analysis. *Prog. Electromagn. Res. M*, **3** (2008), 153–164.
- [10] Hosseini, S.A.; Atlasbaf, Z.; Forooghi, K.: Two new loaded compact planar ultra-wideband antennas using defected ground structures. *Prog. Electromagn. Res. B*, **2** (2008), 165–176.
- [11] Gao, G.P.; Yang, X.X.; Zhang, J.S.: A printed volcano smoke antenna for UWB and WLAN communications. *Prog. Electromagn. Res. Lett.*, **4** (2008), 55–61.
- [12] Lotfi, N.A.A.: Ultra wideband rose leaf microstrip patch antenna. *Prog. Electromagn. Res.*, **86** (2008), 155–168.
- [13] Lin, S.; Yang, S.; Fathy, A.E.; Elsherbini, A.: Development of a novel UWB Vivaldi antenna array using SIW technology. *Prog. Electromagn. Res.*, **90** (2009), 369–384.

- [14] Chen, D.; Cheng, C.H.: A novel compact ultra-wideband (UWB) wide slot antenna with via holes. *Progr. Electromagn. Res.*, **94** (2009), 343–349.
- [15] Rajabi, M.; Mohammadi, M.; Komjani, N.: Simulation of ultra wide-band microstrip antenna using EPML-TLM. *Progr. Electromagn. Res. B*, **2** (2008), 115–124.
- [16] Fortino, N.; Dauvignac, J.Y.; Kossiavas, G.; Staraj, R.: Design optimization of UWB printed antenna for omnidirectional pulse radiation. *IEEE Trans. Antennas Propag.*, **56** (2008), 1875–1881.
- [17] Zaker, R.; Ghobadi, C.; Nourinia, J.: A modified microstrip-fed two-step tapered monopole antenna for UWB and WLAN applications. *Progr. Electromagn. Res.*, **77** (2007), 137–148.
- [18] Abbosh, A.M.; Bialkowski, M.E.; Mazierska, J.; Jacob, M.V.: A planar UWB antenna with signal rejection capability in the 4–6 GHz band. *IEEE Microw. Wirel. Compon. Lett.*, **16** (2006), 278–280.
- [19] Zhang, G.M.; Hong, J.S.; Wang, B.-Z.: Two novel band-notched UWB slot antennas fed by microstrip line. *Progr. Electromagn. Res.*, **78** (2008), 209–218.
- [20] Fallahi, R.; Kalteh, A.A.; Roozbahani, M.G.: A novel UWB elliptical slot antenna with band-notched characteristics. *Progr. Electromagn. Res.*, **82** (2008), 127–136.
- [21] Hong, C.Y.; Ling, C.W.; Tarn, I.Y.; Chung, S.J.: Design of a planar ultrawideband antenna with a new band-notch structure. *IEEE Trans. Antennas Propag.*, **55** (2007), 3391–3397.
- [22] Computer Simulation Technology (CST) Studio Suite, Version 2013.
- [23] Lin, W.-P.; Chao-Hsiang, H.: Coplanar waveguide-fed rectangular antenna with an inverted-I stub for ultrawideband communications. *IEEE Antennas Wirel. Propag. Lett.*, **8** (2009), 228–231.
- [24] Joseph, S.; Paul, B.; Mridula, S.; Mohanan, P.: A novel planar fractal antenna with CPW-feed for multiband applications. *Radioengineering*, **22** (2013), 1262–1266.



**Wessam Zayd Shareef** was born in Baghdad, Iraq in 1981. He received the B.Sc. degree from the University of Baghdad, Department of Mechatronics Engineering. After he finished his first degree in 2004, he had worked with Al-naba'a for Communications and Security Systems Company as Maintenance Engineer from 2005 to 2007. He received his M.Sc. from Universiti Putra Malaysia, Malaysia in 2010. Currently, he is working as a RF Planning Engineer at

Asiacell, Iraq. His main research interests include RF/microwave devices design, and planar technologies and applications.



**Alyani Ismail** received her B.Eng. (Hons) from the University of Huddersfield, in 1999, her M.Sc. and Ph.D. from the University of Birmingham, in 2001 and 2006, respectively. She subsequently became a Lecturer in Universiti Putra Malaysia (UPM) in 2006 and now works as an Associate Professor at the Department of Computer and Communication Systems Engineering, Faculty of Engineering, UPM. She has been appointed to various administrative positions – Deputy Director of Centre for Academic Development, 2012 – now and Head of Department of Computer and Communication Systems Engineering, 2010 – February 2012. Alyani is an active member of IEEE and she served as an Executive Committee for IEEE AP/MTT/EMC Chapter. Alyani specializes in the development of RF and microwave devices particularly passive filters, antennas, and sensors. In recognition of her contributions in research, Alyani has been awarded the Young Excellent Researcher Award for 2010 by the university.



**Adam R.H. Alhawari** was born in Jordan. He acquired the B.Sc. degree in Communication Engineering from Hij-jawi Faculty for Engineering Technology of Yarmouk University, Jordan in 2003. He had an internship program done for couple of months in Cairo, Egypt for Industrial Training of his B.Sc. Meanwhile the M.Sc. and the Ph.D. degrees were both pursued later in 2009 and 2012, respectively, in Wireless Communications Engineering from Universiti Putra Malaysia, Malaysia. That was after a double 2-year duration working in Jordan and then Saudi Arabia. Currently, he is a Senior Lecturer at the Department of Computer and Communication Systems Engineering, Universiti Putra Malaysia since December, 2012. His main research interests are in metamaterial antennas, microwave absorbers, and RFID.